Journal of Materials Chemistry A

PAPER

View Article Online
View Journal | View Issue

Cite this: J. Mater. Chem. A, 2015, 3, 2176

Core–shell structured Ce_2S_3@ZnO and its potential as a pigment†

Wen-Xin Mao,[ab] Wei Zhang,[b] Zi-Xiang Chi,[b] Rong-Wen Lu,*[a] An-Min Cao*[b] and Li-Jun Wan*[b]

Received 29th October 2014
Accepted 25th November 2014

DOI: 10.1039/c4ta05797j

www.rsc.org/MaterialsA

The potential use of cerium selenide (Ce_2S_3) as a non-toxic pigment has long been plagued by its release of hydrogen sulfide (H_2S). Here, it is shown that a uniform nanoshell of zinc oxide (ZnO) can effectively eliminate the released H_2S and also improve the thermal stability of Ce_2S_3. Through a series of investigations, a 40 nm thick ZnO surface coating layer was found to provide full protection for the Ce_2S_3 core, and this thickness is best for eliminating the release of H_2S. Such a core–shell configuration has great potential for real applications of Ce_2S_3 as an odorless and non-toxic inorganic pigment.

Introduction

For many decades, core–shell nanostructures have attracted considerable research interest because of their unique physicochemical properties.[1–5] Generally, the introduction of a surface coating layer can selectively modify the properties of the core materials, leading to an optimized performance of both the core and the shell. Not surprisingly, the core–shell nanostructures can easily find broad applications in a variety of areas, including biology, catalysis, conversion devices and energy storage.[6–11] For example, a recent report showed that a surface coating layer of carbon can be quite effective at preventing photocorrosion of cadmium sulfide.[12] Accordingly, a stable photocatalyst can be successfully prepared. Meanwhile, a surface layer made up of a solid oxide is well known for its capability to improve the thermal stability of its central core materials.[13,14]

Inorganic pigments have been widely used in a multitude of industries such as ceramics, paints, and plastics. However, these commercially or artistically important pigments usually contain highly toxic heavy metals, such as cadmium selenide in Cadmium Red and palladium chromate in Chrome Orange. There is, therefore, an emerging need to develop new types of inorganic pigments without the use of hazardous heavy metals, especially when stricter regulations are now being enforced on traditional pigments.[15–17] Rare earth-based inorganics are another possible source of alternative pigments that have been recently explored. For example, Ce_2S_3 has been identified as a very promising candidate to replace cadmium and organic red pigments because of its non-toxicity and bright colour.[18] Unfortunately, however, pigments containing rare earth sulfides tend to be oxidized and release hydrogen sulfide (H_2S). Both long exposure to moisture and high temperature treatment during the injection moulding of pigments produce the unpleasant smell of H_2S, which is a considerable challenge for the practical application of rare earth sulfides. There have, recently, been preliminary efforts to introduce a silicon dioxide (SiO_2) coating on Ce_2S_3 in order to facilitate the applications of this sulfide, and an enhanced thermal stability has been identified.[19,20] However, the deleterious effects of H_2S release has hardly been addressed because of the inertness of SiO_2 for H_2S adsorption. To alleviate this problem, different absorbents have been used as additives in the pigments.[21,22] Zinc oxide (ZnO) emerges as a good choice because of its high sensitivity to H_2S.[23–25] Equally importantly, both ZnO and its reaction product zinc sulfide have a light color so that it will not tint the original pigment.[26]

A core–shell configuration with an inner core of Ce_2S_3 surrounded by a uniform ZnO nanoshell should best protect the Ce_2S_3. In contrast to relatively poor absorption of H_2S for Ce_2S_3 and ZnO combined in a simple mixture, which is usually the form used for commercially available Ce_2S_3 pigments, H_2S released from Ce_2S_3 in the interior of a core–shell configuration can be absorbed instantaneously by the surrounding ZnO nanoshell without the risk of it diffusing out, leading to a possible total elimination of H_2S. The amount of ZnO needed to totally remove H_2S can thus, be reduced because it is being used more effectively. In this way, the influence of ZnO on the colour of Ce_2S_3 can be minimized. Interestingly, despite the obvious advantages of core–shell structures, a literature survey finds no reports on the construction and evaluation of ZnO nanoshells for an improved performance of Ce_2S_3 pigments.

[a]State Key Laboratory of Fine Chemicals, Dalian University of Technology, Dalian 116024, P. R. China. E-mail: lurw@dlut.edu.cn

[b]Key Laboratory of Molecular Nanostructure and Nanotechnology and Beijing National Laboratory for Molecular Sciences, Institute of Chemistry, Chinese Academy of Sciences (CAS), Beijing 100190, P. R. China. E-mail: anmin_cao@iccas.ac.cn; wanlijun@iccas.ac.cn

† Electronic supplementary information (ESI) available. See DOI: 10.1039/c4ta05797j

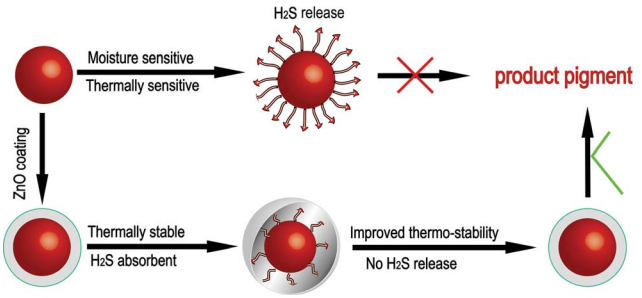

Scheme 1 The advantage of a core–shell configuration of Ce_2S_3@ZnO. The ZnO nanoshell can effectively eliminate the released H_2S from Ce_2S_3 and also improve its thermal stability, leading to a more favorable pigment.

In the present research, an easy synthesis route was adopted to construct a Ce_2S_3@ZnO core–shell nanostructure. A uniform and conformal ZnO surface layer was successfully deposited around the core Ce_2S_3, forming an effective absorption layer for H_2S without an obvious degradation of the pigment colour. The preliminary results show that such a core–shell structure can, not only achieve a total absorption of H_2S, but also improve the thermal stability of the Ce_2S_3 core. The increased relative amount of thermally stable pigment with a minimized H_2S release shows good promise for practical applications of this core–shell structure. Scheme 1 shows the procedure that was used to coat a uniform ZnO nanolayer on Ce_2S_3 core particles.

Results and discussion

The formation of Ce_2S_3@ZnO composites is illustrated in Scheme 1. A synthesis route developed by Yang *et al.* was used, in which ascorbic acid was selected as an effective ligand and stabilizer to control the gradual formation of ZnO on different metals.[27] It was found that this methodology could be transferred well to the coating procedure for Ce_2S_3. A pH value of 6.0 was used to prevent etching of the Ce_2S_3 substrate. Fig. 1a shows a scanning electron microscopy (SEM) image of the pristine Ce_2S_3 sample that was used (denoted as p-Ce_2S_3). The p-Ce_2S_3 is primarily observed as big chunks of particles with irregular shapes. High-resolution SEM reveals that the surfaces of these particles are not smooth, and there exist smaller particles stacked together (inset in Fig. 1a). After the coating treatment, an obvious change in the particle shape was not observed. However, the SEM image in Fig. 1b as well as the HRSEM in the inset of Fig. 1b did reveal that the surfaces of these particles became relatively smooth upon being treated. The development of a surface layer after the coating process was clearly revealed using transmission electron microscopy (TEM). The bare Ce_2S_3 is highly crystalline on the surface with characteristic lattice fringes (ESI Fig. S1b†). After coating, a distinct nanoshell forms as shown in Fig. 1c, circling around the inner particle. The shell thickness was measured and was found to be uniformly 40 nm and the high resolution TEM investigation shows that the shell is actually composed of randomly distributed nanocrystallites with diameters of about 3 nm (ESI Fig. S1d†). The lattice spacing

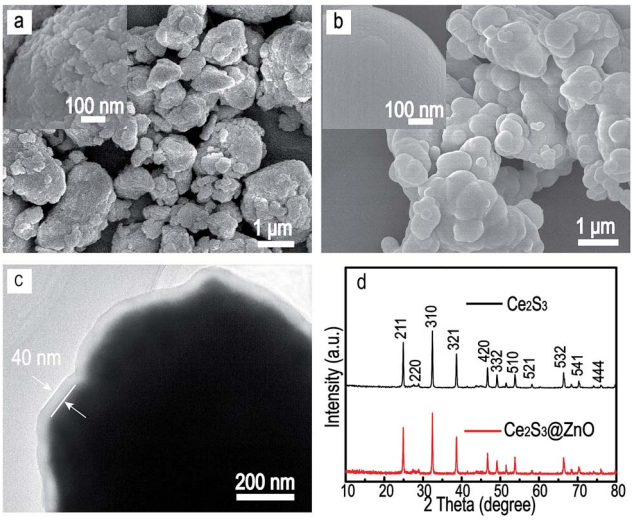

Fig. 1 (a) SEM image of Ce_2S_3 pigment. (b) SEM image of Ce_2S_3@ZnO. (c) TEM image of Ce_2S_3@ZnO with a uniformly 40 nm thick ZnO layer. (d) XRD pattern of Ce_2S_3 and Ce_2S_3@ZnO.

of a randomly selected nanocrystallite was 0.26 nm, which is consistent with the distance between (002) planes of the ZnO structure.[28] The X-ray diffraction (XRD) characterization of the Ce_2S_3 samples before and after coating did not show obvious peaks from ZnO itself (Fig. 1d), which is probably because of the small crystal size and the very small amount of ZnO (5.43 wt%) in the sample.[29,30]

To further reveal the existence of ZnO on the surface, a detailed elemental analysis was carried out on the core–shell structured sample. Fig. 2a shows the energy dispersive spectroscopy (EDS) pattern collected for a representative particle, whose morphology is shown in Fig. 2b. This microanalysis technology clearly reveals the existence of ZnO in the Ce_2S_3 sample. Elemental mapping of this sample (Fig. 2c–f) further shows the locations of the different elements. The well-defined spatial distribution confirms that Ce_2S_3 is fully wrapped by ZnO, forming a typical core–shell Ce_2S_3@ZnO structure. A thorough SEM investigation combined with the elemental analysis of the different particles did not find separate particles of ZnO, indicating that all the ZnO exists as the surface shell without phase separating into independent particles.

The protocol used to synthesize the core–shell particle gives us the capability to easily tune the shell thickness by simply adjusting the concentrations of the reactants. Fig. 3a shows a typical TEM image of a thinner ZnO nanoshell when less zinc acetate (4 mM as compared to 10 mM for the 40 nm thick coating) was used. This shell was determined to have a thickness of only 12 nm, yet still formed a continuous layer on the surface. The corresponding SEM image (ESI Fig. S2†) shows a smoother surface than that of the p-Ce_2S_3. The granular surface underneath is still discernible because the coating is thinner. Also, nanoshells thicker than 40 nm can be prepared by either increasing the amount of zinc acetate or using a seeded growth route. Fig. 3b shows an 80 nm thick ZnO shell prepared by using 20 mM zinc acetate. However, because of the colour difference

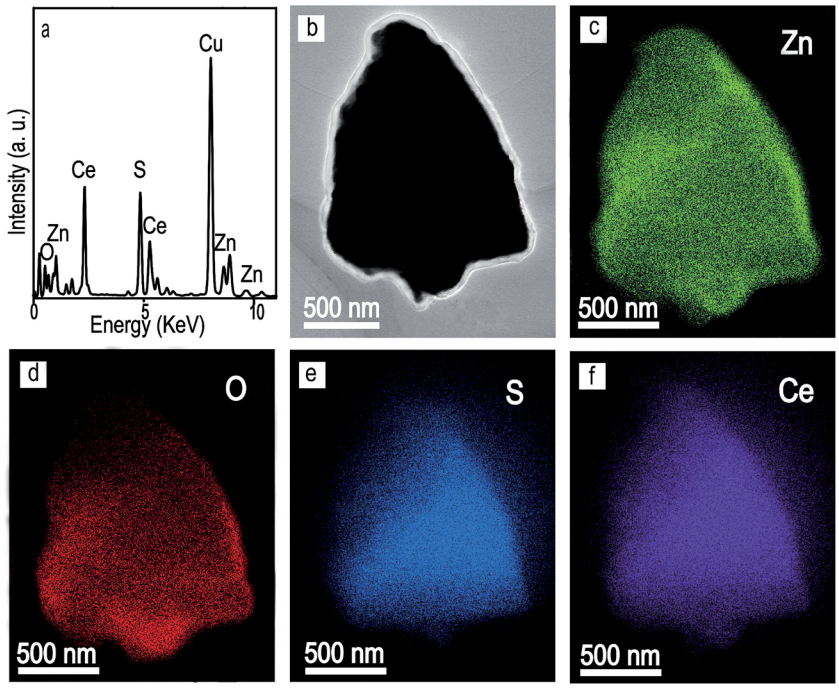

Fig. 2 (a) EDS pattern and (b) TEM image of Ce_2S_3@ZnO. The elemental mapping images of Ce_2S_3@ZnO NP for the elements (c) Zn, (d) O, (e) S and (f) Ce.

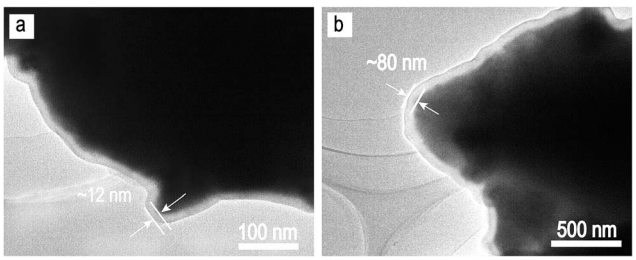

Fig. 3 TEM images of (a) Ce_2S_3@ZnO with a 12 nm thick ZnO shell, and of (b) Ce_2S_3@ZnO with an 80 nm thick ZnO shell.

between ZnO and Ce_2S_3, formation of a nanoshell that was too thick, was found to be detrimental to the colour of the pigment, as is shown in Fig. 7d.

The existence of a uniform shell can provide an ideal shield for the protection of Ce_2S_3. Typically, such a coating layer can contribute to improving the thermal stability of the p-Ce_2S_3. As shown in Fig. 5a, the different samples were treated at 380 °C to reveal their susceptibility to higher temperatures. The p-Ce_2S_3, which is bright red at room temperature, quickly became grey after heating. The XRD pattern identified the formation of CeO_2, which was because of the oxidation of Ce_2S_3 (Fig. 5b). To demonstrate the advantage of the core–shell structure, a commercial sample consisting of a mixture of Ce_2S_3 and ZnO (denoted as Ce_2S_3–ZnO in ESI Fig. S3†) was also tested. No obvious improvement in the thermal stability with ZnO as a separate phase was noticed. Furthermore, the colour became grey after the heat treatment and CeO_2 showed up as the major product. In contrast, for the core–shell structured Ce_2S_3@ZnO with the 40 nm thick layer, the red colour remained nearly intact, which is encouraging. Its XRD pattern did not show an obvious change after heating, suggesting a much better thermal stability in the presence of the ZnO nanoshells. The better thermal stability of our Ce_2S_3@ZnO sample (40 nm thick coating) was also revealed by the thermogravimetry analysis (TGA). As shown in Fig. 4, the weights of p-Ce_2S_3 and commercial Ce_2S_3–ZnO increased during the heating process, which was attributed to the oxidation of Ce_2S_3.[20] In contrast, the Ce_2S_3@ZnO sample did not show this trend, which indicated the obvious contribution of the ZnO nanoshell. Note that a weight loss starting from 350 °C was

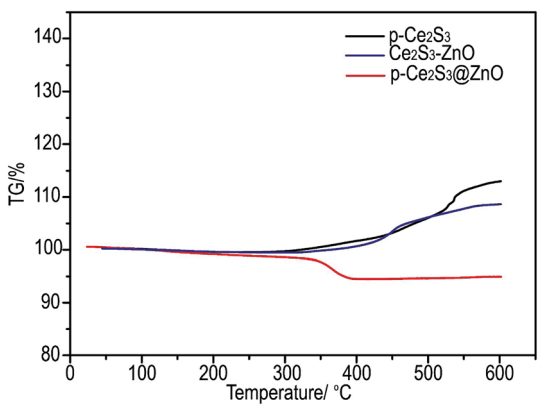

Fig. 4 TGA results of different samples: black line for p-Ce_2S_3; blue line for Ce_2S_3–ZnO and red line for p-Ce_2S_3@ZnO with a 40 nm thick ZnO layer.

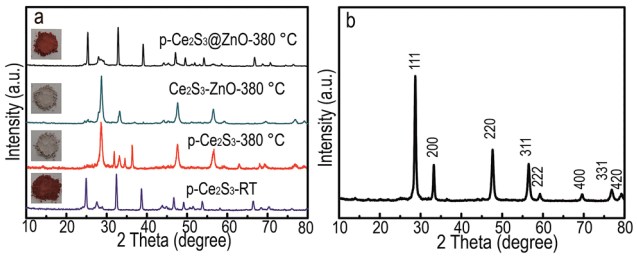

Fig. 5 XRD patterns of (a) different materials after calcination at 380 °C for 2 h. (b) CeO_2.

observed for this core–shell structure, which was probably because of the loss of the ascorbic acid ligand attached to the ZnO nanoparticles.[27]

For the previously mentioned samples with different configurations, systematic tests were performed to evaluate the effect of ZnO on H_2S removal. For the p-Ce_2S_3, it is not surprising that the amount of H_2S released continued to increase with increasing temperature (Fig. 6). Actually, it was very easy to smell the malodorous H_2S gas when the Ce_2S_3 sample was being unpacked after a period of storage (*e.g.*, 2 h in a sealed condition). The introduction of a thin coating layer (12 nm, see TEM image shown in Fig. 3a) helped to remove the H_2S. Not surprisingly, a thicker ZnO nanoshell was better at absorbing H_2S: the sample with a 40 nm thick ZnO shell showed very encouraging results and a total removal of H_2S. For comparison, we measured the amount of H_2S released from the commercial sample of Ce_2S_3–ZnO, which is also capable of eliminating the H_2S gas because of the existence of a large amount of ZnO (8.89 wt%) in the sample. However, as the temperature was increased to 150 °C, an H_2S signal did emerge. In contrast, for the Ce_2S_3@ZnO core–shell structured sample there was no escape of H_2S, and its level remained under the detection limit of the instrument. It was also noted that the ZnO content in Ce_2S_3@ZnO is 5.43 wt%, only 61.52% of that of the commercial Ce_2S_3–ZnO. It emerges that a uniform ZnO nanoshell can not only contribute to the thermal stability, but can also effectively enhance the H_2S control of Ce_2S_3 pigment with much less ZnO.

Inspired by the promising performance of Ce_2S_3@ZnO, a preliminary experiment using injection moulding was carried out to show its possible applications for producing plastics (Fig. 7). The process was carried out at a high temperature of 200 °C. For the p-Ce_2S_3, the injection moulding was very unpleasant for the operator, because of the continuous release of H_2S at 200 °C, which prevents the actual practical use of p-Ce_2S_3 in real conditions. The 40 nm thick ZnO resolves this problem well with no smell of H_2S. The molded plate produced using this ZnO shows no obvious difference from that of p-Ce_2S_3. A change in the plate colour is noticeable when the thickness of the ZnO layer is increased to 80 nm (Fig. 7d). Although the colour of the powder itself did not show a huge change, this difference was magnified because only a small amount of pigment powder was used, as is generally the case for the practical industrial operation. Good control of the content of ZnO proves to be significant, and the sample with a 40 nm thick shell is the best choice for quality of the pigment. The chromaticity data are shown in Table 1. It can be clearly seen that the Ce_2S_3@ZnO samples with 12 nm and 40 nm thick ZnO layers and the original Ce_2S_3 pigment show rather little difference in chromaticity (L^*, a^*, b^* difference is approximately 1 for all).[31,32] However, when the thickness of the ZnO layer was increased to 80 nm, the chromaticity performance exhibited an obvious decrease compared to that of the original Ce_2S_3 pigment (ΔL^*: 3.17, Δa^*: 4.21, Δb^*: 3.03).

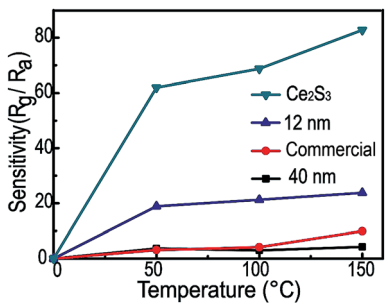

Fig. 6 H_2S absorption curves of different materials.

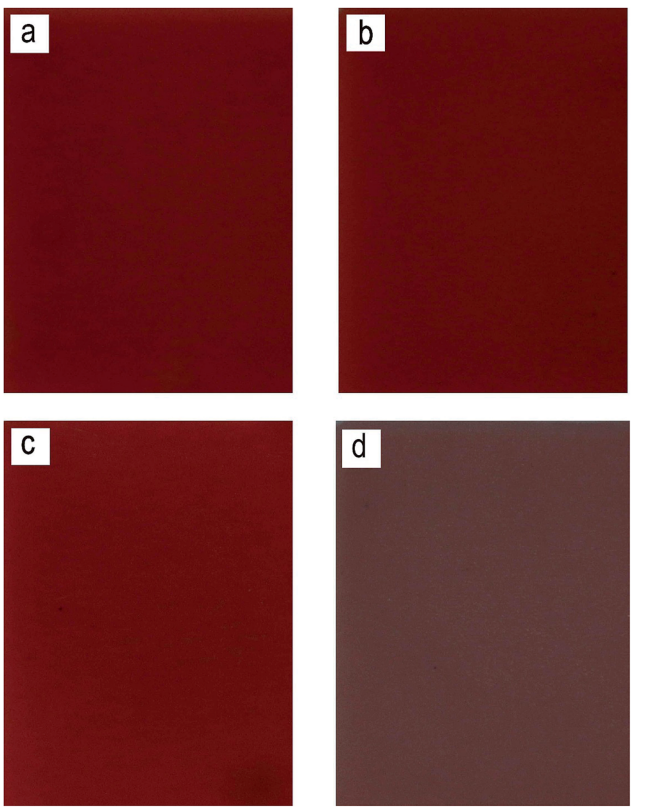

Fig. 7 Plastics made using an injection moulding process with different pigment powders: (a) p-Ce_2S_3, (b) Ce_2S_3@12 nm ZnO, (c) Ce_2S_3@40 nm ZnO, (d) Ce_2S_3@80 nm.

Table 1 The chromaticity of the original Ce_2S_3 and Ce_2S_3@ZnO with different thicknesses of ZnO layer

	Ce_2S_3	Ce_2S_3@ZnO 12 nm shell	Ce_2S_3@ZnO 40 nm shell	Ce_2S_3@ZnO 80 nm shell
L^*	43.46	43.18	42.57	40.29
a^*	43.77	43.10	42.85	39.56
b^*	31.36	30.86	30.44	28.33

Conclusion

In summary, a core–shell structured Ce_2S_3@ZnO was developed to facilitate the application of Ce_2S_3 as an inorganic pigment. By means of an easy, solution-based synthesis route, a uniform and conformal ZnO nanoshell was deposited onto the Ce_2S_3 substrate with a coating thickness that can be readily tuned. A detailed investigation identified that a 40 nm thick ZnO surface coating can provide full protection for the Ce_2S_3 core and eliminate its H_2S release, leading to an odorless powder with much improved thermal stability. Thus, this core–shell structure should improve the potential for the realistic application of Ce_2S_3 as a non-toxic inorganic pigment.

Acknowledgements

This work was supported by the major State Basic Research Program of China (973 program: 2013CB934000, 863 program: 2013AA030800), the National Natural Science Foundation of China (Grant no. 21373238), National Natural Science Foundation of China (Grant no. 21176038), the Chinese Academy of Sciences (XDA09010001). The authors thank the Key Laboratory for Micro-/Nano-Optoelectronic Devices of Ministry of Education, School of Physics and Electronics, Hunan University for the systematic tests to evaluate the contribution of ZnO on H_2S removal and the Beijing Renhe Master Batch Technology Development Center for performing the injection moulding.

References

1 R. Ghosh Chaudhuri and S. Paria, *Chem. Rev.*, 2011, **112**, 2373–2433.
2 F. Caruso, *Adv. Mater.*, 2001, **13**, 11–15.
3 A. H. Lu, E. L. Salabas and F. Schuth, *Angew. Chem., Int. Ed.*, 2007, **46**, 1222–1244.
4 Z. C. Sun, E. Zussman, A. L. Yarin, J. H. Wendorff and A. Greiner, *Adv. Mater.*, 2003, **15**, 1929–1933.
5 P. Reiss, M. Protiere and L. Li, *Small*, 2009, **5**, 154–168.
6 M.-C. Daniel and D. Astruc, *Chem. Rev.*, 2003, **104**, 293–346.
7 Q. Zhang, I. Lee, J. B. Joo, F. Zaera and Y. Yin, *Acc. Chem. Res.*, 2012, **46**, 1816–1824.
8 X. Xia, J. Tu, Y. Zhang, X. Wang, C. Gu, X.-b. Zhao and H. J. Fan, *ACS Nano*, 2012, **6**, 5531–5538.
9 F. Tao, M. E. Grass, Y. W. Zhang, D. R. Butcher, J. R. Renzas, Z. Liu, J. Y. Chung, B. S. Mun, M. Salmeron and G. A. Somorjai, *Science*, 2008, **322**, 932–934.
10 Y. Lu, Y. Mei, M. Drechsler and M. Ballauff, *Angew. Chem., Int. Ed.*, 2006, **45**, 813–816.
11 L. F. Cui, R. Ruffo, C. K. Chan, H. L. Peng and Y. Cui, *Nano Lett.*, 2009, **9**, 491–495.
12 Y. Hu, X. Gao, L. Yu, Y. Wang, J. Ning, S. Xu and X. W. Lou, *Angew. Chem., Int. Ed.*, 2013, **52**, 5636–5639.
13 S. H. Joo, J. Y. Park, C.-K. Tsung, Y. Yamada, P. Yang and G. A. Somorjai, *Nat. Mater.*, 2009, **8**, 126–131.
14 C.-H. Tsai, S.-Y. Chen, J.-M. Song, I.-G. Chen and H.-Y. Lee, *Corros. Sci.*, 2013, **74**, 123–129.
15 S. Hirai, K. Shimakage, Y. Saitou, T. Nishimura, Y. Uemura, H. Mitomo and L. Brewer, *J. Am. Ceram. Soc.*, 1998, **81**, 145–151.
16 M. A. Perrin and E. Wimmer, *Phys. Rev. B: Condens. Matter Mater. Phys.*, 1996, **54**, 2428–2435.
17 I. G. Vasilyeva, B. M. Ayupov, A. A. Vlasov, V. V. Malakhov, P. Macaudiere and P. Maestro, *J. Alloys Compd.*, 1998, **268**, 72–77.
18 J. M. Tomczak, L. V. Pourovskii, L. Vaugier, A. Georges and S. Biermann, *Proc. Natl. Acad. Sci. U. S. A.*, 2013, **110**, 904–907.
19 G. H. Chen, Z. F. Zhu, H. Liu, Y. F. Wu and C. K. Zhu, *J. Rare Earths*, 2013, **31**, 891–896.
20 S. Y. Yu, D. R. Wang, Y. Liu, Z. Li, X. F. Zhang, X. N. Yang, Y. F. Wang, X. J. Wang and H. Q. Su, *RSC Adv.*, 2014, **4**, 23653–23657.
21 N. Yamazoe, *Sens. Actuators, B*, 1991, **5**, 7–19.
22 Z. Sun, H. Yuan, Z. Liu, B. Han and X. Zhang, *Adv. Mater.*, 2005, **17**, 2993–2997.
23 J. Goclon and B. Meyer, *Phys. Chem. Chem. Phys.*, 2013, **15**, 8373–8382.
24 K. X. Yao and H. C. Zeng, *J. Phys. Chem. C*, 2007, **111**, 13301–13308.
25 M. S. Wagh, L. A. Patil, T. Seth and D. P. Amalnerkar, *Mater. Chem. Phys.*, 2004, **84**, 228–233.
26 L. Dloczik, R. Engelhardt, K. Ernst, S. Fiechter, I. Sieber and R. Konenkamp, *Appl. Phys. Lett.*, 2001, **78**, 3687–3689.
27 Y. Yang, S. H. Han, G. J. Zhou, L. J. Zhang, X. L. Li, C. Zou and S. M. Huang, *Nanoscale*, 2013, **5**, 11808–11819.
28 H. Zeng, W. Cai, P. Liu, X. Xu, H. Zhou, C. Klingshirn and H. Kalt, *ACS Nano*, 2008, **2**, 1661–1670.
29 N. R. Jana, H.-h. Yu, E. M. Ali, Y. Zheng and J. Y. Ying, *Chem. Commun.*, 2007, 1406–1408.
30 L. Qian, Y. Zheng, J. Xue and P. H. Holloway, *Nat. Photonics*, 2011, **5**, 543–548.
31 M. Jansen and H. P. Letschert, *Nature*, 2000, **404**, 980–982.
32 D. L. MacAdam, *J. Opt. Soc. Am.*, 1943, **33**, 18–26.

